

# How to Tune the Alumina Aerogels Structure by the Variation of a Supercritical Solvent. Evolution of the Structure During Heat Treatment

S. A. Lermontov,<sup>\*,†,‡</sup> E. A. Straumal,<sup>†,‡</sup> A. A. Mazilkin,<sup>§</sup> I. I. Zverkova,<sup>§</sup> A. E. Baranchikov,<sup>||</sup>  
B. B. Straumal,<sup>§,⊥,#</sup> and V. K. Ivanov<sup>||</sup>

<sup>†</sup>Department of Chemistry, Moscow State University, 1, Leninskie Gory 119991 Moscow, Russia

<sup>‡</sup>Institute of Physiologically Active Compounds, Russian Academy of Sciences, 1 Severnii pr., 142432 Chernogolovka, Russia

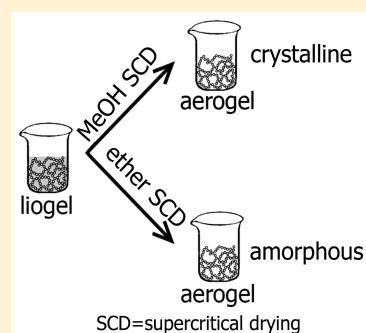
<sup>§</sup>Institute of Solid State Physics, Russian Academy of Sciences, 2 Ossipyana str., 142432 Chernogolovka, Russia

<sup>||</sup>Kurnakov Institute of General and Inorganic Chemistry, Russian Academy of Sciences, 31 Leninskii prosp., 119991 Moscow, Russia

<sup>⊥</sup>National University of Science and Technology «MISIS», 4 Leninskii prosp., 119049 Moscow, Russia

<sup>#</sup>Moscow Institute of Physics and Technology (State University), 9 Institutskii per., 141700 Dolgoprudny, Russia

**ABSTRACT:** Alumina aerogels are obtained by supercritical drying (SCD) in four solvents of different chemical natures. The phase transformations, the morphological changes, and the thermal stability during heat treatment in the range 20–1200 °C are investigated. The as-prepared samples obtained by SCD in MeOH are identified as crystalline aluminum hydroxide methoxide, and those obtained by SCD in *i*-PrOH consist of alumina with small size of crystallite grains. In contrast to alcohol-dried samples, the initial ether-dried aerogels are amorphous (as determined by X-ray diffraction). Calcination of the samples causes their crystallization and recrystallization. After heat treatment at 1200 °C, all samples consisted only of the  $\alpha$ -alumina phase. TEM study demonstrated that the nature of the solvent used for SCD significantly affects the morphology of the aerogels. Low-temperature nitrogen adsorption investigation of the aerogel samples confirms the influence of the nature of supercritical fluid (SCF) on the structure of the aerogels. Moreover, the nature of SCF affects both the specific surface area and its evolution during heat treatment.



## 1. INTRODUCTION

Aerogels are unique materials having a low density, a high porosity, and a large specific surface area. The preparation of aerogels is a multistage process, which includes gel synthesis by a sol–gel method, aging and washing in an appropriate solvent followed by supercritical drying (SCD). Due to their properties, aerogels can be used as effective thermal<sup>1–3</sup> and acoustical insulators,<sup>4</sup> sorbents,<sup>5,6</sup> catalyst supports,<sup>7,8</sup> and so on.

It is generally assumed that alumina aerogels are capable of providing thermal insulation over a temperature range larger than more common silica aerogels and can serve as a useful material for several applications.<sup>9</sup> High-surface-area aluminas are widely used as catalysts, catalyst supports, and sorbents.<sup>10,11</sup> Moreover, micro- and nanocrystalline aluminas are also widely applied as precursor materials for Al<sub>2</sub>O<sub>3</sub>-based ceramics.<sup>12</sup>

The influence of solvents used for SCD on aerogel properties is still poorly understood. Tajiri et al. reported the effects of SCF (methanol, ethanol, 2-propanol, and CO<sub>2</sub>) on the properties of silica aerogels.<sup>13</sup> They found that samples prepared by SCD in alcohols were covered by the corresponding alkyl groups. In our previous papers,<sup>14–16</sup> we demonstrated that the specific surface area in SiO<sub>2</sub>, Al<sub>2</sub>O<sub>3</sub>, and ZrO<sub>2</sub> aerogels depended considerably on the solvent used for

SCD. This work is focused on the influence of the nature of SCD on the structure and the phase composition of alumina aerogels and their structural evolution during heat treatment. This investigation aims to reveal the possibility to reliably control the chemical and phase composition, the porosity, and the surface area of alumina aerogels during their synthesis.

## 2. EXPERIMENTAL SECTION

In this paper we use the following notation: MeOH, *i*-PrOH, Et<sub>2</sub>O, and MTBE samples are dried using methanol, isopropanol, diethyl ether, and *tert*-butyl methyl ether, respectively, as a supercritical fluid.

**2.1. Alumina Aerogels Synthesis.** Aluminum nitrate, Al(NO<sub>3</sub>)<sub>3</sub>·9H<sub>2</sub>O (Aldrich, 99+%), propylene oxide (Aldrich, 99.5%), isopropyl alcohol (Aldrich, 99.5+%), methanol (Aldrich, 99.8%), diethyl ether, and *tert*-butyl methyl ether (Aldrich, 99%) were used in the as-received state. Alumina sols were prepared according to the method described in ref 17. Al(NO<sub>3</sub>)<sub>3</sub>·9H<sub>2</sub>O (4.6 g, 0.0123 mol) was dissolved in 20 mL of

Received: October 26, 2015

Revised: January 4, 2016

Published: January 30, 2016

isopropanol and propylene oxide (7.83 g, 0.135 mol) was then added. The reaction mixture was stirred for 2 min and transferred to plastic molds, which were sealed by Parafilm, and the solutions were allowed to gelate at room temperature. Gel formation typically occurred within 10–15 min. Then the gels were aged at room temperature for 24 h. Samples were washed by soaking five times using the solvent mentioned above, and the solvents were exchanged daily with fresh solvents. After being washed, the aerogels were dried under supercritical conditions in the same solvents.

SCD was performed as follows. Liogel (gel before drying) samples were put into a stainless steel autoclave ( $V \approx 40$  mL). The autoclave was filled with a solvent ( $V \approx 20$  mL) and heated. The system was heated to a temperature of 15–20 °C above the critical point of the solvent. The heating rate was approximately 50 °C/h. The critical point is 235 °C for *i*-PrOH, 239 °C for MeOH, 193 °C for Et<sub>2</sub>O, and 224 °C for MTBE. When the required temperature was reached (the pressure in the autoclave was 20–22 MPa for all solvents), the valve was opened and the pressure decreased down to the ambient value in 2 h. The autoclave was then evacuated in 20–30 min (2–5 mmHg), cooled to room temperature, and opened. Moreover we have prepared some additional samples which were dried at a temperature significantly exceeding the critical, i.e., we prepared alumina aerogel samples by the SCD in Et<sub>2</sub>O and MTBE at 270 °C. These samples were prepared to identify the effect of drying temperature on the structure of the samples.

Each aerogel sample was divided into several parts and then they were annealed in a muffle furnace in an air atmosphere at 300, 500, 800, 1000, and 1200 °C for 24 h. The 700 and 900 °C annealing points were additionally carried out for *i*-PrOH samples. The furnace was heated to the required temperature at a rate of approximately 5 °C/min.

**2.2. Investigation Methods.** The specific surface area of the aerogels was determined by measuring low-temperature nitrogen adsorption with an ATX-06 analyzer using the 8-point BET method. X-ray diffraction (XRD) analysis was carried out on a SIEMENS D-500 diffractometer (Cu  $K\alpha_1$  radiation). The grain size was estimated using the Powder Cell software package. The Scherrer equation was used to estimate the crystallite grain size in case when no crystal structure with known positions of atoms could be attributed to the lines in X-ray profile. The microstructure of the obtained samples was examined on a JEM-2100 transmission electron microscope at an accelerating voltage of 200 kV.

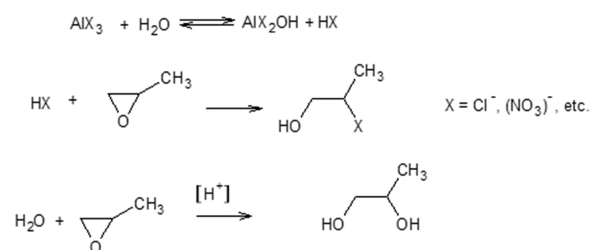
The simultaneous TGA/DSC analysis was performed on TA Instruments SDT Q-600 (250 mL·min<sup>-1</sup> air flow, constant heating rate mode at 10 °C·min<sup>-1</sup>) up to 1200 °C. A sample weight was approximately 10 mg.

### 3. RESULTS AND DISCUSSION

The convenient and mild epoxide-based procedure proposed by Simpson<sup>18</sup> was used for alumina aerogel preparation. This procedure is based on the ability of alkene oxides to scavenge acids irreversibly, facilitating slow and controlled aluminum salts hydrolysis (Scheme 1).

A 3-fold excess of the epoxide compound is used because of the acid catalyzed side reaction of alkene oxide with water, which does not remove acid from the reaction mixture. The hydroxylated aluminum species condense further to form a solid phase, an alumina gel, which is then transformed into aerogel by SCD.

#### Scheme 1. Chemistry of Epoxide Facilitated Aluminum Salt Hydrolysis



**3.1. Transmission Electron Microscopy.** Figure 1 shows the results of TEM investigation of the as-prepared aerogel samples. The TEM images show that the materials consist of an interconnected network of nanometer-sized particles.

It is clearly seen that the microstructure of the samples depends on the solvent used for SCD (Figure 1)

The *i*-PrOH sample consists of agglomerated regions with an irregular shape (Figure 1a). The size of these regions is about 7 nm. In the dark-field TEM image of *i*-PrOH sample (Figure 1b) crystallite particles are observed. Their size is approximately 2 nm.

The MeOH sample consists of fibrous regions with a fiber diameter of 4–7 nm and various fiber lengths. The fibers are interconnected and form a tangled structure (see the representative fibrous structure in Figure 1c). A similar fibrous morphology is commonly reported for the alumina materials prepared from alkoxide precursors.<sup>9,17,19,20</sup> The crystallite size can be clearly seen in a dark-field image (Figure 1d). The individual crystallites are about 4 nm in diameter and have irregular shape.

The ether samples (both Et<sub>2</sub>O and MTBE samples) are composed of interconnected spherical regions with a diameter of 2–8 nm (Figure 1e,g). Such a “colloidal” type of microstructure is typical of for many main group and transition metal oxide aerogel materials.<sup>17</sup> Small spherical crystallites approximately 1 nm in diameter are visible in a dark-field TEM image of the ether sample (Figure 1f,h).

**3.2. X-ray Diffraction.** The results of XRD analysis also demonstrates that the structure and the phase composition of the aerogel samples depends on the solvent used for SCD. Results of the XRD measurements are collected in the Table 1.

All samples can be divided into two groups, namely ether (Et<sub>2</sub>O and MTBE) samples and alcohol (MeOH and *i*-PrOH) samples.

Figure 2 shows the X-ray diffraction patterns of the MTBE and Et<sub>2</sub>O samples in the as-prepared state and after the annealing at 500, 800, 1000, and 1200 °C respectively. The XRD patterns of Et<sub>2</sub>O samples do not differ from those of the MTBE aerogels.

The as-prepared ether samples are amorphous (as determined by XRD). Their fwhm (full width at half-maximum) is about 12° and annealing at 300 °C does not change this state. When the calcination temperature increases up to 500 °C, crystallization of the samples begins and a cubic phase appears in the structure (PDF 00–074–2206). The spectrum of the sample annealed at 500 °C contains broad diffraction peaks, which demonstrate a crystalline structure with small grain size of the material. When the annealing temperature increases, the XRD peaks gradually become narrower. The sample annealed at 1000 °C has a clearly defined crystalline structure of the cubic Al<sub>2</sub>O<sub>3</sub> compound

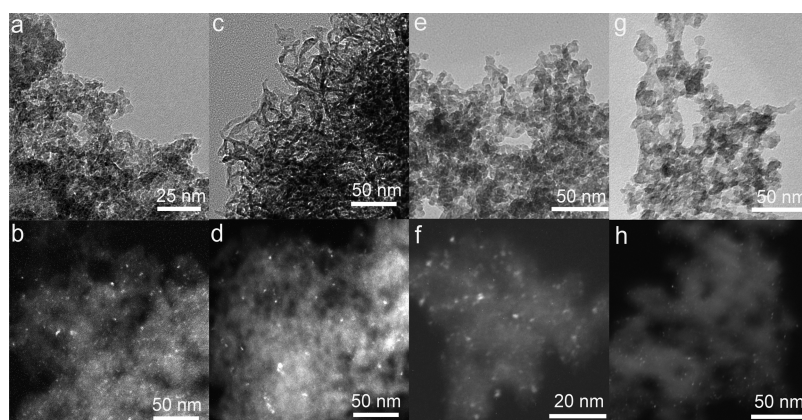


**Figure 1.** TEM images of as-prepared i-PrOH (a and b), MeOH (c and d), MTBE (e and f), and Et<sub>2</sub>O (g and h) samples; a, c, e, and g are bright field images and b, d, f, and h are dark field images, respectively.

**Table 1. Systematization of Phase Composition for the Alumina Aerogels Samples Depending on the Annealing Temperature<sup>a</sup>**

	i-PrOH	MeOH	Et <sub>2</sub> O	MTBE
as-prepared	C	Al-H-M	A	A
300	C	Al-H-M	A	A
500	C	Al-H-M + T	C	C
700	C			
800	C	T	C	C
900	C			
1000	R+C+M	T	C	C
1200	R	R	R	R

<sup>a</sup>Letters A, C, M, T, and R denote amorphous, cubic (00-074-2206), monoclinic (00-035-0121), tetragonal (00-046-1131), and rhombohedral (00-046-1212) alumina phases, respectively. Al-H-M means aluminum hydroxide methoxide (00-022-1538).

(PDF 00-074-2206) with a grain size of about 4 nm. A further increase in the temperature gives rise to recrystallization of the sample. The sample annealed at 1200 °C contains  $\alpha$ -Al<sub>2</sub>O<sub>3</sub> crystallites with a rhombohedral lattice (PDF 00-046-1212). The sample annealed at 1200 °C is well crystallized as its fwhm is about 0.18°, which is comparable to the fwhm of the standard sample.

In contrast to the ether aerogels, the as-prepared alcohol samples have a fine-grained crystalline structure and their phase composition is different for the MeOH and i-PrOH aerogels.

The X-ray diffraction peaks of the initial i-PrOH sample are rather broad. Nevertheless, peak widths (FWHM is about 6.5°) do not allow us to call the sample amorphous (Figure 3b). These peaks correspond to the alumina compound with a cubic lattice (PDF 00-074-2206). The grain size of crystalline aluminum oxide is about 2 nm, which is in good agreement with TEM data. Annealing of the i-PrOH sample at 300 °C does not change the phase composition. No recrystallization of the sample is observed when the calcination temperature increases 700 °C. The diffraction peaks become narrower, indicating the formation of a structure with a larger grain size. According to our estimations, the grain size increases to 4 nm.

In the diffraction pattern of the i-PrOH samples annealed at 700 °C a peak from another alumina phase (PDF 00-035-0121) appears at  $2\theta \approx 32.8^\circ$ . This peak is the highest peak of this phase according to the PDF data. Its appearance means that phase formation begins at this temperature.

At a calcination temperature of 1000 °C, we observed the entire set of diffraction lines of this monoclinic phase. After annealing at this temperature, the i-PrOH sample consisted of a mixture of the following three phases: cubic alumina (PDF 00-074-2206), monoclinic alumina (PDF 00-035-121), and rhombohedral  $\alpha$ -alumina (PDF 00-046-1212). It should also

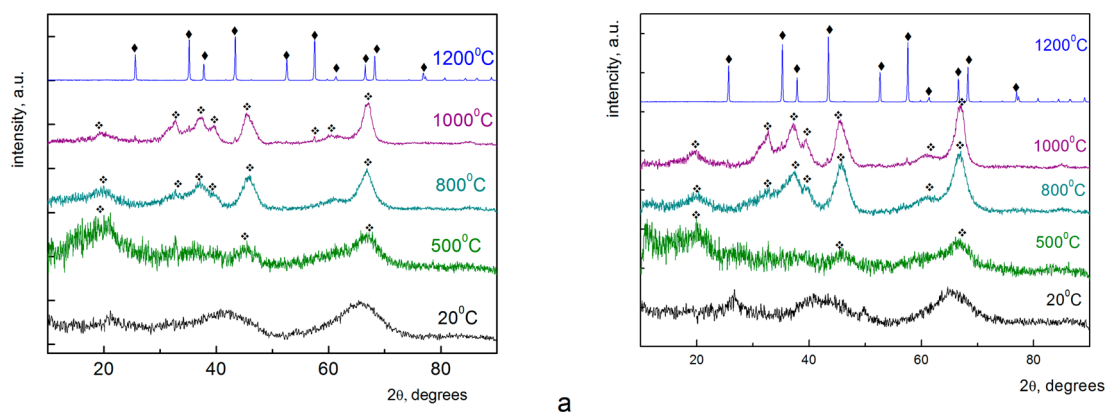


**Figure 2.** XRD patterns for MTBE- (a) and Et<sub>2</sub>O- (b) samples for the as-prepared sample and annealed samples. The phases detected in the samples are denoted as follows: four diamonds, cubic alumina (00-074-2206), one diamond,  $\alpha$ -alumina (00-046-1212). Only the most intensive peaks are denoted in the sake of clarity.



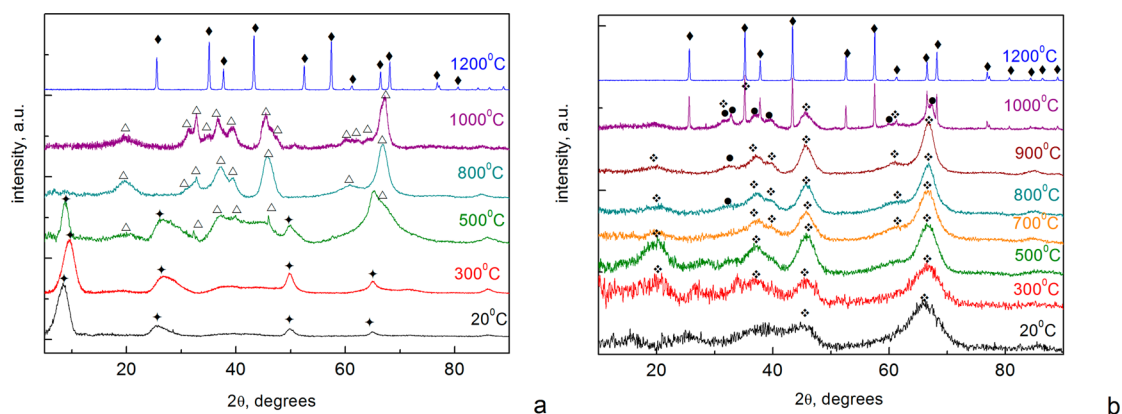


**Figure 3.** X-ray diffraction patterns for MeOH (a) and *i*-PrOH samples (b), annealed at various temperatures. The phases detected in the samples are denoted as follows: curved-sided diamond, aluminum hydroxide methoxide (00-022-1538);  $\Delta$ , tetragonal alumina (00-046-1131); four diamonds, cubic alumina (00-074-2206);  $\bullet$ , monoclinic alumina (00-035-0121); and  $\blacklozenge$ ,  $\alpha$ -alumina (00-046-1212). Only the most intensive peaks are denoted in the sake of clarity.

be noted that FWHMs of these three phases are different. Rhombohedral  $\alpha$ -alumina is well crystallized. fwhm of cubic phase is still considerably larger than the instrumental broadening and the grain size is estimated to be about 5 nm. As to the monoclinic phase, its fwhm is not so large and its grain size is about 23 nm. The X-ray diffraction pattern of the *i*-PrOH sample annealed at 1200 °C contained only the reflections from the well-crystallized  $\alpha$ -alumina phase (PDF 00-046-1212).

The phase composition of the MeOH samples differs from that for others aerogels. According to the X-ray diffraction pattern in Figure 3a the as-prepared MeOH sample consists of aluminum hydroxide methoxide ( $\text{AlO}(\text{OH})_{0.5}(\text{OCH}_3)_{0.5}$ ) (PDF 00-022-1538). The grain size of this phase (approximately 4 nm) was estimated by the Scherrer equation. It should be noted that the formation of this phase was predictable. It is known<sup>21</sup> that the addition of methanol to an aqueous solution of sodium aluminate at 60 °C leads to the formation of aluminum hydroxide methoxide.

When the annealing temperature reaches 500 °C, a new phase forms. The X-ray diffraction pattern of the MeOH samples calcined at 500 °C contains peaks of aluminum hydroxide methoxide phase and very broad peaks of another phase. The peak widths complicate identification of the phase composition of this sample; nevertheless, the tetragonal alumina compound (PDF 00-046-1131) gives the best fit to the set of diffraction peaks. The relative peak intensities of aluminum hydroxide methoxide phase, i.e., its volume fraction, decrease in comparison with the MeOH samples annealed at a lower temperature. With a further increase in the calcination temperature, the diffraction peaks become narrower. The MeOH samples annealed at 800 and 1000 °C contain the tetragonal alumina phase (PDF 00-046-1131). The XRD patterns of the MeOH samples annealed at 1200 °C and those of the samples dried in other solvents demonstrate the presence of only  $\alpha$ -alumina phase (PDF 00-046-1212).

All samples annealed at 1200 °C are well crystallized as its fwhm is about 0.18°, which is comparable to the fwhm of the standard sample. It means that it is not correct to estimate the crystallite size by the peak broadening. Thus, we have calculated the  $\alpha$ -alumina grain size by means of TEM. Figure 4 demonstrate the microstructure of the  $\text{Et}_2\text{O}$  sample annealed at 1200 °C. TEM measurements gave us the grain size value  $\sim$ 220 nm (see Figure 4).

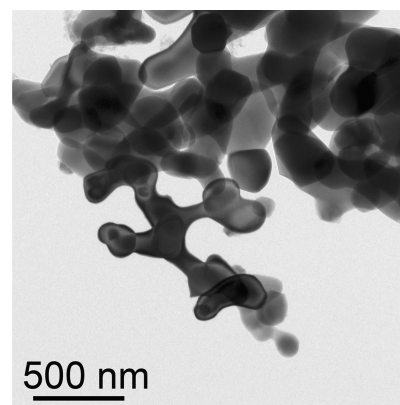


**Figure 4.** TEM image of  $\text{Et}_2\text{O}$  sample annealed at 1200 °C.

As was previously described, SCD was performed in different supercritical fluids (MeOH, *i*-PrOH,  $\text{Et}_2\text{O}$ , and MTBE) at 255, 250, 215, and 240 °C, respectively. As was shown by XRD, the phase composition of the ether samples differed from that of the alcohol samples. Specifically, the ether samples are amorphous (as determined by XRD) and the alcohol samples have a fine-grained crystalline nature. This difference can be explained by two factors: different drying temperatures and different natures of a supercritical fluid. Additional experiments were carried out to reveal the decisive crystallization factor for our samples. We performed SCD in both ethers at 270 °C, which is even higher than the SCD temperature in alcohols. The X-ray diffraction patterns of these samples are shown in Figure 5. It is clearly seen that the diffraction maxima are extremely wide for both samples (fwhm is approximately 11.5°), revealing their amorphous nature. Hence, it can be concluded that the nature of solvent rather than the drying temperature is the decisive factor of crystallization in our samples.

Alcohols are much more polar solvents compared to aprotic ethers. They can efficiently solvate both cations and anions facilitating a redissolution–reprecipitation processes and leading to the formation of a crystalline structure. Therefore, both alcohol samples are crystalline with small grains and both ether samples are amorphous. It should also be mentioned that methanol and *i*-PrOH differ significantly in their solvating ability. It is known that the solubility of  $\text{SiO}_2$  in methanol is an order of

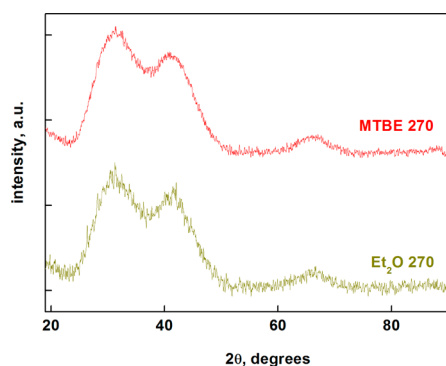


**Figure 5.** X-ray diffraction patterns of Et<sub>2</sub>O and MTBE samples dried at 270 °C.

magnitude higher than that in other alcohols.<sup>22</sup> Based on this fact, the solubility of Al<sub>2</sub>O<sub>3</sub> in methanol is expected to be higher than that in *i*-PrOH. We believe that the increased solubility in methanol makes it possible to form a crystalline structure with the largest crystal size.

**3.3. Low Temperature Nitrogen Adsorption.** BET curves are shown in Figure 6.

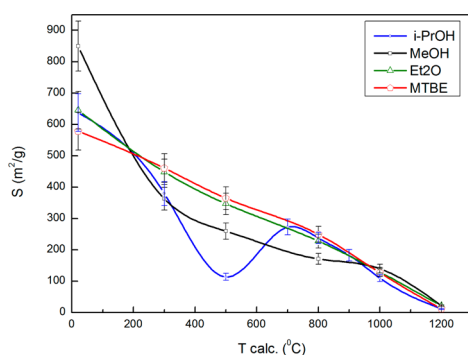


**Figure 6.** BET curves for the *i*-PrOH, MeOH, Et<sub>2</sub>O, and MTBE samples annealed at various temperatures.

It is obvious from Figure 6 that the BET curves can be divided into two groups. The ether and MeOH samples demonstrate a monotonic decrease in the specific surface area with increasing calcination temperature. The BET curve of the *i*-PrOH samples differs from the other curves. An increase in the calcination temperature for the *i*-PrOH samples to 500 °C is accompanied by a substantial decrease in the specific surface area. Unlike other samples, a further increase in the temperature leads to a local maximum at approximately 850–900 °C.

It was shown earlier (see XRD data) that recrystallization of the *i*-PrOH sample occurred in the same temperature region. The results published in ref 23 revealed that the recrystallization of Al<sub>2</sub>O<sub>3</sub> can result in a decrease in the grain size which implies an increase in the specific surface area. This process is likely to cause the local maximum in the BET curve of the *i*-PrOH sample.

**3.4. Thermal Analysis.** The data of thermal analysis of the aerogels prepared by SCD in all solvents are presented in Figure 7. It follows from the TGA curves that the sample mass loss occurs at two stages. The first stage is extended to 200 °C and corresponds to the remove of physically bound water and organic solvents (alcohols and ethers). During the second stage

(between 200 and 600 °C), slow oxidation of chemically bonded organic substances takes place.

The process of removing of the volatiles (water and organic solvents) adsorbed on the aerogel surface is typically characterized by an endothermic peak in DSC curves. However, in our case, we did not observe a significant endothermic peak in this temperature range. This fact can be explained by a small amount of adsorbed solvents and water and by the overlapping of this endothermic effect with the more intense exothermic peak corresponding to the oxidation of chemically bonded organic substances. Let us conventionally denote it further on as an oxidation peak. Now we consider thermal analysis data for each sample in detail.

MeOH samples exhibit an oxidation peak at  $T \approx 340$  °C. The weight loss in the temperature range evidence the oxidation of organic substances. However, XRD analysis data show that an annealing temperature above 300 °C is the onset of recrystallization of MeOH aerogel, when the AlO(OH)<sub>0.5</sub>(OCH<sub>3</sub>)<sub>0.5</sub> phase is substituted by the tetragonal alumina phase. Thus, the peak in the DSC curve at 340 °C can be referred to both oxidation and recrystallization.

In the DSC curves for *i*-PrOH samples, we observed several exothermic peaks at 330, 440, 823, and a minor peak at 1100 °C. The peaks at low temperatures (330 and 440 °C) can be attributed to oxidation peaks. The two remaining peaks correspond to recrystallization observed by means of XRD, i.e., the appearance of the monoclinic phase at 800 °C and crystallization with the formation of  $\alpha$ -alumina at 1200 °C.

Three exothermic peaks at 337, 845, and 1100 °C were observed in the DSC curve of MTBE samples. The very broad peak with a maximum at 800 °C corresponds to the formation of cubic alumina. This finding correlates well with the XRD data. According to the XRD spectra, cubic alumina forms in the temperature range 300–1000 °C. Clear reflections of this crystal structure are observed for the samples annealed at 800 °C. The exothermic peak at 1100 °C corresponds to the phase transition from cubic alumina to rhombohedral  $\alpha$ -alumina.

Two DSC peaks at 345 and 790 °C are observed for Et<sub>2</sub>O samples. As in the previous cases, the first peak is attributed to oxidation and the beginning of crystallization. As in the case of the MTBE sample, the maximum at 790 °C corresponds to completion of the formation of cubic alumina. In addition to these two broad peaks, a narrow intense exothermic peak at 245 °C is seen. Dialkyl ethers, but not MTBE, are known to form peroxides easily (Scheme 2).<sup>24</sup> Therefore, this peak can be explained by the thermal decomposition of diethyl ether peroxide formed due to the oxidation of adsorbed Et<sub>2</sub>O by atmospheric oxygen.

#### 4. CONCLUSIONS

Alumina aerogels were prepared by SCD in solvents of different chemical natures. The influence of various SCFs on the properties of aerogel was investigated. The phase transformations, the morphological changes, and the thermal stability of alumina aerogels during heat treatment were investigated. The as-prepared ether aerogels were identified by XRD as amorphous materials. The phase transformations within the annealing temperature range 20–1200 °C were as follows: amorphous aerogel alumina with a cubic lattice (PDF 00-074-2206),  $\alpha$ -alumina (PDF 00-046-1212). The initial MeOH samples were identified as aluminum hydroxide methoxide (PDF 00-022-1538). The phase transformation path in the range 20–1200 °C for MeOH was as follows:

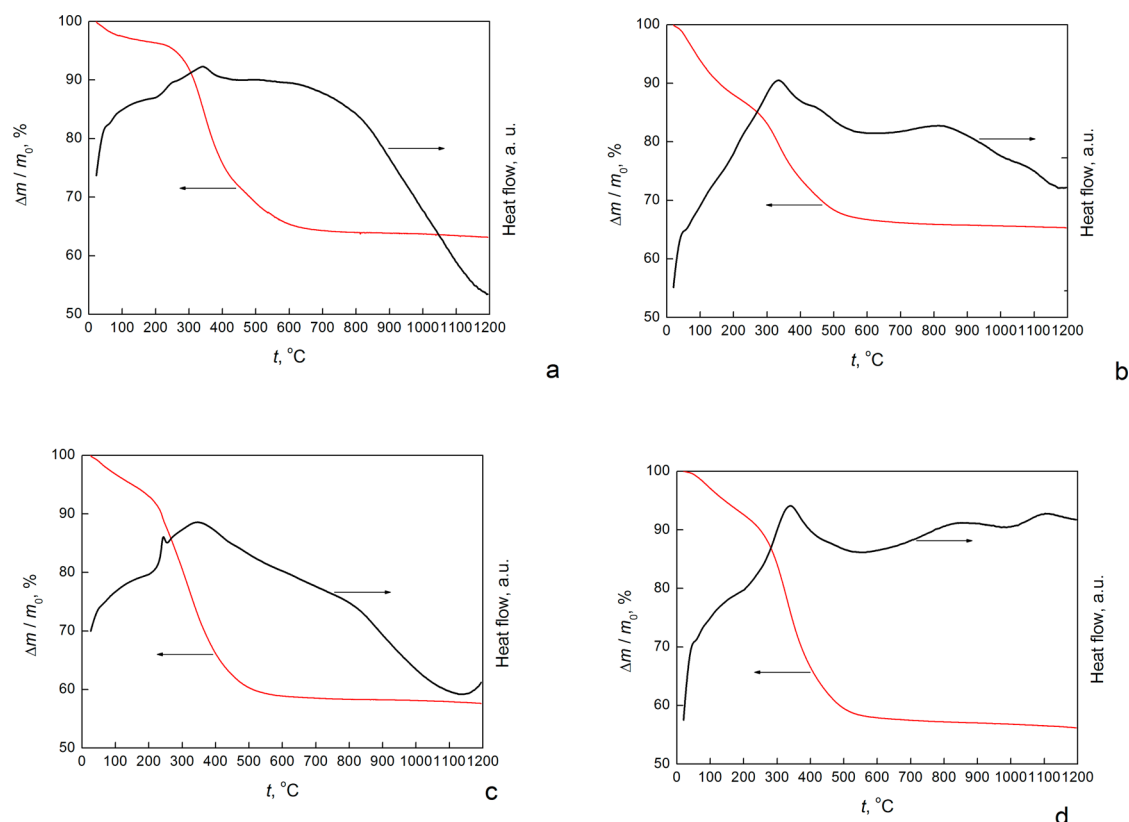
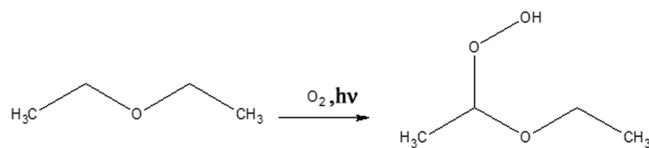


**Figure 7.** Thermal analysis data (TGA and DSC) for the alumina aerogel samples dried in MeOH (a), iPrOH (b), Et<sub>2</sub>O (c), and MTBE (d).

### Scheme 2. Oxidation of Diethyl Ether by Atmospheric Oxygen



aluminum hydroxide methoxide (PDF 00-022-1538), mixture of two phases, namely, aluminum hydroxide methoxide (PDF 00-022-1538) and tetragonal alumina phase (PDF 00-046-1131), tetragonal alumina phase (PDF 00-046-1131),  $\alpha$ -alumina (PDF 00-046-1212). The as-prepared i-PrOH samples were identified as crystalline alumina with small grains of cubic lattice (PDF 00-074-2206). The phase transformations during annealing were as follows: alumina with cubic lattice (PDF 00-074-2206), mixture of two phases (PDF 00-074-2206 and PDF 00-035-0121), mixture of several phases, namely, alumina with a cubic lattice (PDF 00-074-2206), rhombohedral  $\alpha$ -alumina (PDF 00-046-1212) and monoclinic alumina (PDF 00-035-0121),  $\alpha$ -alumina phase (PDF 00-046-1212).

The observed variety of the phase transformations is thought to be caused by different solubility of alumina liogels in supercritical fluids of different nature.

The investigation of aerogel samples by low-temperature nitrogen adsorption confirms the influence of the nature of SCF on the structure of aerogels. It was shown that the nature of SCF affects both the specific surface area and its evolution during heat treatment.

Therefore, the main structural characteristics of the prepared aerogels were shown to be adjusted by changing the nature of the SCD solvent.

### AUTHOR INFORMATION

#### Corresponding Author

\*E-mail: [lermon@ipac.ac.ru](mailto:lermon@ipac.ac.ru). Fax: +74965249508. Tel: +74965242587.

#### Notes

The authors declare no competing financial interest.

### ACKNOWLEDGMENTS

This work was supported by the Russian Scientific Foundation (Grant No. 14-33-00017). The authors are grateful to Olga Shakhlevich for the help with the XRD measurements.

### REFERENCES

- (1) Yoldas, B. E.; Annen, M. J.; Bostaph, J. Chemical Engineering of Aerogel Morphology Formed under Nonsupercritical Conditions for Thermal Insulation. *Chem. Mater.* **2000**, *12*, 2475–2484.
- (2) Husing, N.; Schubert, U. Aerogels Airy Materials: Chemistry, Structure, and Properties. *Angew. Chem., Int. Ed.* **1998**, *37*, 23–45.
- (3) Fricke, J.; Lu, X.; Wang, P.; Buttner, D.; Heinemann, U. Optimization of Monolithic Silica Aerogel Insulants. *Int. J. Heat Mass Transfer* **1992**, *35*, 2305–2309.
- (4) Conroy, J. F. T.; Hosticka, B.; Davis, S. C.; Smith, A. N.; Norris, P. M. Microscale Thermal Relaxation During Acoustic Propagation in Aerogel and Other Porous Media. *Microscale Thermophys. Eng.* **1999**, *3*, 199–215.
- (5) Hrubesh, L. W. Aerogel Applications. *J. Non-Cryst. Solids* **1998**, *225*, 335–342.
- (6) Aristov, Y. I.; Restuccia, G.; Tokarev, M. M.; Cacciola, G. Selective Water Sorbents for Multiple Applications, 10. Energy Storage Ability. *React. Kinet. Catal. Lett.* **2000**, *69*, 345–353.
- (7) Antczak, T.; Mrowiec-Bialon, J.; Bielecki, S.; Jarzelski, A. B.; Malinowski, J. J.; Lachowski, A. I.; Galas, E. Thermostability and Esterification Activity of Mucor Javanicus Lipase Entrapped in Silica

Aerogel Matrix and in Organic Solvents. *Biotechnol. Tech.* **1997**, *11*, 9–11.

(8) Pierre, M.; Buisson, P.; Fache, F.; Pierre, A. Influence of the Drying Technique of Silica Gels on The Enzymatic Activity of Encapsulated Lipase. *Biocatal. Biotransform.* **2000**, *18*, 237–251.

(9) Poco, J. F.; S, J. H.; Hrubesh, L. W. Synthesis of High Porosity, Monolithic Alumina Aerogels. *J. Non-Cryst. Solids* **2001**, *285*, 57–63.

(10) Euzen, P.; Raybaud, P.; Krokidis, X.; Toulhoat, H.; Le Loarer, J. L.; Jolivet, J. P. *Handbook of Porous Solids*; Wiley-VCH: Weinheim, Germany, 2002.

(11) Bermudez, V. M. Computational Study of Environmental Effects in the Adsorption of DMMP, Sarin, and VX on Gamma-Al<sub>2</sub>O<sub>3</sub>: Photolysis and Surface Hydroxylation. *J. Phys. Chem. C* **2009**, *113*, 1917–1930.

(12) Hudson, L. K.; Misra, C.; Wefers, K. *Industrial Inorganic Chemicals and Products*; Wiley-VCH: Weinheim, Germany, 1999.

(13) Tajiri, K.; Igarashi, K.; Nishio, T. Effects of Supercritical Drying Media on Structure and Properties of Silica Aerogel. *J. Non-Cryst. Solids* **1995**, *186*, 83–87.

(14) Lermontov, S. A.; Malkova, A. N.; Yurkova, L. L.; Straumal, E. A.; Gubanova, N. N.; Baranchikov, A. E.; Ivanov, V. K. Diethyl and Methyl-tert-butyl Ethers as New Solvents for Aerogels Preparation. *Mater. Lett.* **2014**, *116*, 116–119.

(15) Lermontov, S. A.; Malkova, A. N.; Yurkova, L. L.; Straumal, E. A.; Gubanova, N. N.; Baranchikov, A. E.; Smirnov, M.; Tarasov, V. I.; Buznik, V. M.; Ivanov, V. K. Hexafluoroisopropyl Alcohol as a New Solvent for Aerogels Preparation. *J. Supercrit. Fluids* **2014**, *89*, 28–32.

(16) Lermontov, S. A.; Sipyagina, N. A.; Malkova, A. N.; Yarkov, A. V.; Baranchikov, A. E.; Kozik, V. V.; Ivanov, V. K. Functionalization of Aerogels by the Use of Pre-Constructed Monomers: the Case of Trifluoroacetylated (3-aminopropyl) Triethoxysilane. *RSC Adv.* **2014**, *4*, 52423–52429.

(17) Baumann, T. F.; Gash, A. E.; Chinn, S. C.; Sawvel, A. M.; Maxwell, R. S.; Satcher, J. H. Synthesis of High-Surface-Area Alumina Aerogels without the Use of Alkoxide Precursors. *Chem. Mater.* **2005**, *17*, 395–401.

(18) Gash, A. E.; Tillotson, T. M.; Satcher, J. H.; Hrubesh, L. W.; Simpson, R. L. New sol-gel Synthetic Route to Transition and Main-Group Metal Oxide Aerogels Using Inorganic Salt Precursors. *J. Non-Cryst. Solids* **2001**, *285*, 22–28.

(19) Mizushima, Y.; Hori, M. Alumina aerogel Catalysts Prepared by 2 Supercritical Drying Methods Used in Methane Combustion. *J. Mater. Res.* **1995**, *10*, 1424–1428.

(20) Carnes, C. L.; Kapoor, P. N.; Klabunde, K. J. Synthesis, Characterization, and Adsorption Studies of Nanocrystalline Aluminum Oxide and a Bimetallic Nanocrystalline Aluminum Oxide/Magnesium Oxide. *Chem. Mater.* **2002**, *14*, 2922–2929.

(21) Chang, T. S.; Na, J. H.; Jung, C. Y.; Koo, S. M. An Easy one-pot Synthesis of Structurally Controlled Aluminum Hydroxide Particles from an Aqueous Sodium Aluminate Solution. *J. Ceram. Process. Res.* **2009**, *10*, 832–839.

(22) Asano, T.; Kitahara, S. The Dissolution of Heat-treated Silica Gel Powders and Change of their Surface Induced by Treatment with Methanol at 150–250°C. *Nippon Kagaku Zasshi* **1970**, *91*, 109–117.

(23) Keysar, S.; Shter, G. E.; deHazan, Y.; Cohen, Y.; Grader, G. S. Heat Treatment of Alumina Aerogels. *Chem. Mater.* **1997**, *9*, 2464–2467.

(24) Kirk-Othmer *Kirk-Othmer Encyclopedia of Chemical Technology*, 4th ed.; Wiley: New York, 1992–1998.